Ex vivo drug response profiling detects recurrent sensitivity patterns in drug resistant ALL

DOI:
10.1182/blood-2016-09-738070

Document Version
Accepted author manuscript

Published in:
Blood

Ex vivo drug response profiling detects recurrent sensitivity patterns in drug resistant ALL

Viktoras Frismantas[1,2,*], Maria Pamela Dobay[3*], Anna Rinaldi[1,2,*], Joelle Tchinda [1,2], Samuel H. Dunn[4], Joachim Kunz[5], Paulina Richter-Pechanska[5], Blerim Marovca[1,2], Orrin Pail[1,2], Silvia Jenni[1,2], Ernesto Diaz-Flores[6], Bill H. Chang[7], Timothy J. Brown[8], Robert H. Collins[8], Sebastian Uhrig[9], Prakash Balasubramanian[9], Obul R. Bandapalli[5], Salome Higi[1,2], Sabrina Eugster[1,2], Pamela Voegeli[10], Mauro Delorenzi[3,11], Gunnar Cario[12], Mignon L. Loh[13], Martin Schrappe[12], Martin Stanulla[14], Andreas E. Kulozik[5], Martina U. Muckenthaler[5], Vaskar Saha[15,16], Julie A. Irving[17], Roland Meisel[18], Thomas Radimerski[19], Arend Von Stackelberg[9,20,21,], Cornelia Eckert[9,20,21], Jeffrey W. Tyner[22], Peter Horvath[23,24], Beat C. Bornhauser[1,2,*] and Jean-Pierre Bourquin[1,2,*]

[1]Department of Oncology, University Children's Hospital Zurich, Zurich, Switzerland

[2]Children's Research Center, University Children's Hospital Zurich, Zurich, Switzerland

[3]SIB Swiss Institute of Bioinformatics, Lausanne, Switzerland

[4]The University of Texas Southwestern Medical School, Dallas, TX, USA

[5]Department of Pediatric Oncology, Hematology and Immunology, University of Heidelberg, Heidelberg, Germany

[6]Department of Pediatrics and Helen Diller Family Comprehensive Cancer Center, University of California-San Francisco, San Francisco, CA, USA

[7]Division of Hematology and Oncology, Department of Pediatrics, Doernbecher Children's Hospital, Oregon Health & Science University, Portland, Oregon

[8]The University of Texas Southwestern Medical Center, Dallas, TX, USA

[9]German Cancer Research Center (DKFZ), Heidelberg, Germany

[10]Institute of Forensic Medicine, University of Zurich, Zurich, Switzerland

[11]Ludwig Center for Cancer Research, University of Lausanne, Lausanne, Switzerland

[12]Department of Pediatrics, University Medical Centre Schleswig-Holstein, Kiel, Germany
[13]Department of Pediatrics, University of California-San Francisco, San Francisco, CA, USA
[14]Department of Pediatric Hematology and Oncology, Hannover Medical School, Hannover, Germany
[15]Division of Molecular & Clinical Cancer Sciences, School of Medical Sciences, Faculty of Biology, Medicine and Health, University of Manchester, Manchester, United Kingdom
[16]Tata Translational Cancer Research Centre, Tata Medical Centre, Kolkata, India
[17]Northern Institute for Cancer Research, Newcastle University, Newcastle upon Tyne, United Kingdom
[18]Division of Pediatric Stem Cell Therapy, Clinic for Pediatric Oncology, Hematology and Clinical Immunology, Medical Faculty, Heinrich Heine University, Düsseldorf, Germany
[19]Disease Area Oncology, Novartis Institutes for BioMedical Research, Basel, Switzerland
[20]Department of Pediatric Oncology/Hematology, Charité Universitätsmedizin Berlin, Germany
[21]German Cancer Consortium (DKTK), Heidelberg, Germany
[22]Department of Cell, Developmental & Cancer Biology, Oregon Health and Science University, Portland, OR, USA
[23]Synthetic and Systems Biology Unit, Hungarian Academy of Sciences, Biological Research Center (BRC), Szeged, Hungary.
[24]Institute for Molecular Medicine Finland, University of Helsinki, Helsinki, Finland.
* equal contribution

Running title: Actionable information by drug response profiling in ALL

Keywords: drug activity profiling, drug resistant acute lymphoblastic leukemia, automated microscopy, BH3-mimetics, precision medicine, dasatinib

Grant Support: This work was supported by the Cancer League of the Canton of Zurich, the Empiris foundation, the foundation “Kinderkrebsforschung Schweiz”, the Sassella foundation,

the “Stiftung für Krebsbekämpfung”, the Swiss National Science Foundation (310030-133108, 310030-156407), the Fondation Panacee, the clinical research focus program “Human Hemato-Lymphatic Diseases” of the University of Zurich, the German Childhood Cancer Foundation and the German Cancer Consortium. P.H. acknowledges support from the Hungarian National Brain Research Program (MTA-SE-NAP B-BIOMAG) and the Finnish TEKES FiDiPro Fellow Grant 40294/13. J.W.T. is supported by The Leukemia & Lymphoma Society, the V Foundation for Cancer Research, the Gabrielle’s Angel Foundation for Cancer Research, and the National Cancer Institute (5R00CA151457-04; 1R01CA183947-01).This research received funding from the European Union’s Seventh Framework Programme for research, technological development, and demonstration (Grant agreement no. 278514 - IntReALL).

Correspondence:

Jean-Pierre Bourquin, jean-pierre.bourquin@kispi.uzh.ch

University Children’s Hospital Zurich

Steinwiesstrasse 75

CH-8032 Zurich, Switzerland

Phone, +41 44 266 7304

Fax, +41 44 266 7171

Disclosure of Potential Conflicts of Interest: T.R. is a full-time employee of Novartis Pharma AG. The remaining authors declare no competing financial interests.

Word count: 3999

Number of figures and tables: 6 figures and 1 table

ABSTRACT

Drug sensitivity and resistance testing on diagnostic leukemia samples should provide important functional information to guide actionable target and biomarker discovery. We provide proof of concept data by profiling 60 drugs on 68 acute lymphoblastic leukemia (ALL) samples mostly from resistant disease in co-cultures on bone marrow stromal cells. Patient-derived xenografts retained the original pattern of mutations found in the matched patient material. Stromal co-culture did not prevent leukemia cell cycle activity, while a specific sensitivity profile to cell cycle related drugs identified samples with higher cell proliferation both *in vitro* and *in vivo* as leukemia xenografts. In cases with refractory relapses, individual patterns of marked drug resistance, but also exceptional responses to new agents of immediate clinical relevance were detected. The BCL2-inhibitor venetoclax was highly active below 10 nM in BCP-ALL subsets including *MLL-AF4* and *TCF3-HLF* ALL, and in some T-ALLs, predicting *in vivo* activity as a single agent and in combination with dexamethasone and vincristine. Unexpected sensitivity to dasatinib with IC50 values below 20 nM was detected in two independent T-ALL cohorts, which correlated with similar cytotoxic activity of the SRC Inhibitor KX2-391 and inhibition of SRC phosphorylation. A patient with refractory T-ALL was treated with dasatinib based on drug profiling information and achieved a five-month remission. Thus, drug profiling captures disease-relevant features and unexpected sensitivity to relevant drugs, which warrants further exploration of this functional assay in the context of clinical trials in order to develop drug repurposing strategies for patients with urgent medical needs.

Key points:

- *Ex vivo* drug profiling captures disease-relevant features and relevant sensitivity to therapeutic agents in ALL
- A subset of resistant T-ALL without mutations in *ABL1* is highly responsive to dasatinib providing a rationale for drug repurposing

INTRODUCTION

The treatment of relapsed and refractory ALL remains challenging[1]. Progress in ALL genomics[2] provides unprecedented insight into potentially actionable targets, such as activating mutations in tyrosine kinases[3], RAS[4] or IL7R[5]. Recurrent features such as *MLL-AF4* rearrangements, the *TCF3-HLF* fusion[6], or hypodiploid karyotypes[4] define rare subgroups with highly resistant disease. However, a majority of patients who may benefit from innovative therapies are still identified based on the persistence of minimal residual disease (MRD)[1,7,8] or remission-induction therapy failure[9].

Large integrative studies on cell line panels illustrate the difficulty of extrapolating drug responses based on genomic data[10,11], even when indicative lesions in druggable pathways occur. Moreover, such alterations may be over- or underrepresented in cell lines, whereas patient-derived xenografts (PDX) appear to reproduce the genetic driver mutation landscape in leukemia more closely[12-14]. To obtain insight into inter-patient drug response heterogeneity, we developed an *in vitro* platform directly using patient-derived leukemia cells. We hypothesized that drug response profiling of ALL even without *a priori* information on genetic lesions or activated pathways will detect sensitivity that may otherwise be overlooked. This approach will complement *in vivo* PDX models, which have obvious limitations in compound coverage and flexibility[15]. Drug sensitivity testing revealed individual drug response phenotypes in AML[16] and identified new strategies to bypass tyrosine kinase inhibitor (TKI) resistance in patients with deleterious BCR-ABL mutations[17]. Conversely, characteristic tyrosine kinase mutations could be predicted based on drug activity[18]. Drug activity patterns can also identify an ALL subtype with tonic pre-BCR signalling[19].

To establish a drug profiling platform, we took advantage of PDX from clinically relevant ALL subgroups[20-24] and based on previous reports[16,18,21-23,25,26], adapted a serum free ALL co-culture system on h-TERT immortalized human bone marrow-derived mesenchymal stromal cells (MSC)[27,28] to an automated microscopic image readout for drug testing. This population-

based approach reveals relevant activity clusters of therapeutic agents, identifying actionable targets that have not yet been exploited in conventional ALL treatment.

MATERIALS AND METHODS

Human samples. Primary human ALL cells were recovered from cryopreserved bone marrow aspirates of patients enrolled in the ALL-BFM 2000, 2009 and ALL-REZ-BFM 2002 studies. Informed consent was given in accordance with the Declaration of Helsinki and the ethics commission of the Kanton Zurich (approval number 2014-0383). Samples were classified as standard-risk (SR), medium-risk (MR), high-risk (HR), or very high-risk (VHR) according to the ALL-BFM 2000 stratification[22], or as relapse (R) and refractory relapse (RR). Patients from a second cohort consented to protocols reviewed by the Institutional Review Boards at Oregon Health & Science University and UT-Southwestern.

Xenograft model. Patient derived xenografts (PDX) were generated as described[23] by intrafemoral injection of $1x10^5$ to $5x10^6$ viable primary ALL cells in NSG mice. Leukemia progression was monitored in the peripheral blood by flow cytometry using anti-mCD45, anti-hCD45, anti-hCD19 or anti-hCD7 antibodies. Xenograft identity was verified by DNA fingerprinting using the commercial AmpFlSTR® NGM SElectT kit.

Genomic characterization of leukemia samples.
Primary patient material and matched xenografts were analysed by targeted sequencing and multiplex ligation-dependent probe amplification (MLPA). In 19 BCP-ALL, cases without an established abnormality (B-other)[29] or targetable kinase-activating lesions[3], fluorescence in-situ hybridization (FISH) was performed (Probes from Cytocell, Cambridge, UK). Detailed protocols are in the supplementary methods section.

***In vitro* drug profiling platform.** Drug responses were assessed in ALL cell co-cultures on hTERT-immortalized primary bone marrow mesenchymal stromal cells (MSC)[20] as described[22] in 384 well plates (Greiner, REF781090). $2.5x10^3$ MSC cells/well were plated

in 30µL AIM-V® medium 24h before adding 2-3x10^4 ALL cells in 27.5µL medium recovered from cryopreserved samples. Compounds were reconstituted in DMSO (10mM stock concentrations) and stored at -80°C. Serially-diluted drugs were prepared using epMotion 5070 and Tecan D300 robots. An independent T-ALL cohort was tested as described in[18].

Drug response quantification and statistical analysis. We used a fitting routine based on the four-parameter log-logistic function (R package drc, version 2.3-96) on data normalized against DMSO-treated samples. Outliers were detected and removed prior to curve fitting by detecting local slope changes with a linear fit. Non-convergent cases were identified based on linear fit parameters. R codes are available under https://github.com/pampernickel/drTools. Hierarchical clustering was performed to group patients according to their drug responses (R package gplots). Differential drug responses of patient groups of interest were evaluated using the non-parametric, Mann-Whitney U-test.

***In vivo* drug treatment.** Venetoclax and combinations: 5-8 mice were transplanted with 1x10^6 ALL cells i.v. per treatment arm. Randomized cohorts were treated with vehicle, 100 mg/kg/day venetoclax (Activebiochem[30]) orally, 10.5 mg/kg dexamethasone (Mepha) i.p. bi-weekly and 0.5 mg/kg Vincristine (Teva) i.p. once a week. Cytarabine, docetaxel and dasatinib: animals (one per condition) were intravenously transplanted with 7x10^6 ALL cells. After five days, animals were treated with 50mg/kg cytarabine (Sandoz) i.p. for five days, 5mg/kg docetaxel (Taxotere) i.v. twice or 50mg/kg dasatinib (Selleck, dissolved as described[31]) orally for five days. Leukemic burden was determined post-treatment by flow cytometry.

Cell assays. Viability: Viability in 2.5x10^4 ALL cells in suspension or co-culture with 2.5x10^3 MSC cells in AIM-V medium was measured by flow cytometry at 1, 4 and 7 days (7-AAD, reported as day 4 mean±SD). Proliferation and apoptosis:1x10^5 ALL cells were seeded with 1x10^4 MSC. Proliferating and apoptotic cells were labelled using the Click-iT EdU Imaging Kit and Cell Event™ Caspase-3/7 Green, respectively. Proliferating and non-proliferating groups were identified with an Expectation-Maximization (EM)-mixture model (R package mixtools).

Intracellular flow cytometry and Western Blot. $10x10^6$ ALL cells were fixed in 2% paraformaldehyde, permeabilized with ice-cold methanol, and indirectly tagged with FITC-labelled antibodies. For Western blots (Bio-Rad Criterion™) whole-cell extracts from $3\text{-}5x10^6$ cells were used. Detailed protocols are in the supplementary methods section.

RESULTS

Drug response profiling reveals distinct clusters of activity in ALL

Co-cultures on hTERT-immortalized MSC[28] facilitate survival of most B-cell precursor (BCP-) and T-ALL cells[21]. This protective effect may even increase the stringency of drug testing[32]. We tested 60 preclinical and clinical compounds (**Table S1**) using an imaging-based cell viability readout[21] (**Figure 1**) on ALL xenografts derived from patients with standard-risk or high-risk ALL based on MRD persistence, and relapsed and refractory ALL. Patient and PDX samples were characterized using established diagnostic workflows, including tests for most recurrent translocations that activate tyrosine kinase pathways (**Table S2A** and **S2B**) and by targeted sequencing of 52 frequently mutated genes in ALL. We retrieved the expected pattern of mutations (**Figure S1**, **Table S3**), with frequent events in *KRAS* (13/25) and *TP53* (10/25), consistent with previous reports[33,34]. On average, 74% of single nucleotide variants (SNVs) and insertions/deletions (indels) were conserved between the primary diagnostic samples and PDX (**Figure 1B**, **Figure S1**). Oncogenic translocations were always maintained. We also included samples from poor- and favourable-risk groups, *TCF3-HLF*- and *TCF3-PBX1*-positive ALL subtypes, for which we recently reported a strong conservation of the genomic landscape in PDX[35].

To evaluate the potential of this ex-vivo platform, we profiled 24 T-ALL and 44 BCP-ALL PDX, derived from pre-treatment diagnostic samples (ALL-BFM-2000 study[36], **Figure 2**). For each drug, we used eight doses, optimized from an initial five-point screen (**Table S4**). None of the tested compounds affected MSC viability at concentrations lethal to ALL cells, indicating selective drug activity (**Figure 2**). Unsupervised clustering of drug responses (shown here as IC50 values) identified various patterns of response. Compounds including anthracyclines, the BH3 mimetic navitoclax (ABT-263) and the proteasome inhibitor bortezomib were effective at low (IC50<10nM) and narrow IC50 range in most cases (cluster A). A second group of agents including the BCL2-specific BH3 mimetic venetoclax[30], tyrosine kinase inhibitors and conventional cytotoxic agents such as glucocorticoids, topoisomerase inhibitors and nucleotide

analogues (gemcitabine, cytarabine) showed responses distributed over a wider concentration range, with high activity in the nanomolar range in some cases and low activity in others (clusters B, C and E). Venetoclax (Cluster C) was generally more active in BCP-ALL, but showed similar activity in a T-ALL subset. In cluster E, we identified two groups of agents, whose separation was driven by differences in response to antimetabolites (cytarabine, gemcitabine), antimitotic drugs (vincristine, docetaxel), the aurora kinase inhibitors AT9283 and barasertib and the Polo-like kinase inhibitor BI-2536. Finally, very strong sensitivity was detected in a few ALL cases for drugs that were otherwise generally not active in ALL on this platform (cluster G). These included SMAC mimetics (e.g. LCL161), an observation which led us to show that a BCP-ALL subset was extremely responsive to SMAC mimetics through RIP1 kinase-dependent necroptosis and apoptosis[37]. The ABL/SRC inhibitor dasatinib is also highly active in a T-ALL subset, which we discuss below. High peak plasma concentrations (Cmax) were reported for most clinical compounds in our panel (**Figure S2**), suggesting that effective concentrations may be achieved *in vivo*. Our platform provides reproducible drug activity profiles that identify functional phenotypes and give new insights for therapeutic targeting. No correlations between drug responses and genetic lesions were found (**Table S5**).

Drug profiling captures leukemia intrinsic differences in cell proliferation and survival

While most ALL samples tested in co-culture survive on MSC, we noticed relative cell survival heterogeneity, suggesting differences in cell proliferation and spontaneous cell death rates across samples (**Figure 3A**). We did not detect ALL migration beneath stromal cells (pseudoemperipolesis) or cobblestone structure-like formation[26] that could interfere with microscopy readouts. Median cell viability on MSCs was 69% of seeded cells for BCP-ALL and 94% for T-ALL, compared to 1.2% and 45.5% in monoculture after 96 hours. A high rate of survival on this platform (viability of >70% at day 3 compared to day 0) correlated with a higher ratio (r>1) of cells in S-phase versus apoptotic cells (**Figure 3A**). To determine whether these differences are due to stromal co-culture effects or intrinsic features of ALL cells, we compared leukemia proliferation and drug sensitivity patterns *ex vivo* and *in vivo* in leukemia xenografts. Marked differences in sensitivity were detected in both BCP- and T-ALL for drugs whose

mechanisms of action require active cycling (**Figure 2** cluster E, **Figure S3**), including mitotic spindle formation inhibitors, DNA synthesis, cell cycle and mitosis regulatory kinases. We used a mixture model fit to distinguish high- (>40% of cells in S-phase) from low- (<40% of cells in S-phase) proliferating ALL cases. ALL samples with high proliferative activity *in vitro* engrafted significantly faster (p-value=0.0008) than samples with low proliferative activity (**Figure 3B**). As expected, drugs with the highest differential activity in high- and low-proliferating samples inhibit targets involved in cell cycle control (**Figure S4**). Most importantly, samples with rapid engraftment kinetics (**Figure 3B**) were more sensitive to cytarabine and docetaxel *ex vivo* (**Figure 3C**), which correlates with stronger anti-leukemic effects *in vivo* (**Figure 3D**). Thus, the *ex vivo* co-culture model captures leukemia-specific characteristics with respect to cell cycle activity, which are preserved *in vivo* in the leukemia xenograft model and are not caused by the co-culture conditions.

As other groups opted for systems based on monocultures, we compared our co-culture data to a readout in serum supplemented liquid leukemia cultures [18]. Selecting 8 BCP-ALL and 19 T-ALL samples, we confirmed improved survival of most of these samples on MSC compared to cell suspension cultures **(Figure S5A-B)**. While IC50 values from co-culture and monoculture were significantly correlated for 22 drugs tested under both conditions (Spearman ρ=0.64, p-value <2.2e^{-16}), there were several discrepancies in drugs of interest. We observed a significant correlation of drug activity in co-cultures with *in-vivo* drug responses (**Figure S5D-F**), most evident for venetoclax (**Figure S5D**), docetaxel and dasatinib, and to a lesser extent for cytarabine (**Figure S5E**). In contrast, drug activity data obtained from liquid monocultures only showed a predictive trend for cytarabine, but not for the other agents tested (**Figure S5F**). These observations support the potential of our system for the identification of relevant vulnerabilities in a clinical setting.

Drug profiling reveals individual patterns of drug sensitivity and resistance in relapsed and refractory ALL

Drug profiling may convey relevant information to select new agents for salvage therapy in patients with highly resistant disease. To compare the activity of different substances in different patients, it is important to evaluate drug activity in a single case against the full response range obtained on the same platform for other leukemia cases, including clinically relevant subsets. We profiled PDX samples of twelve patients with relapsed ALL refractory to salvage therapy (refractory relapse, RR), who did not achieve a second or third remission required for inclusion in early clinical trials (**Figure 4A**), as well as primary leukemia cells from five patients with refractory disease in real time prospectively (**Figure 4B**, **Table 1**). **Figure 4** shows IC50 values for a selection of therapeutic agents in samples of interest against those obtained for all other samples on our platform (grey). RR ALL samples were generally more resistant to agents used for induction in ALL such as dexamethasone (10/12 cases), cytarabine (9/12 cases) and doxorubicin (9/12 cases), compared to other diagnostic and relapse ALL cases (**Figure 4A**). In contrast, individual samples were highly sensitive to dexamethasone, idarubicin and mitoxantrone, which are included in the standard of care for relapsed ALL[38], and to new agents from different classes, such as venetoclax, dasatinib, bortezomib, nutlin, JQ1 and panobinostat. Again, we noticed unexpected responses in a few cases to venetoclax and dasatinib, which we discuss in the next sections. Additionally, sensitivity patterns could be associated with cytogenetic groups. For example, *MLL-AF4* ALL cases were sensitive to PI3K/mTOR/AKT or HSP90 inhibitors, consistent with previous reports[39] (**Figure S6**).

To assess the feasibility of our approach in the clinical setting, we tested five cases with highly refractory ALL at the time of relapse (**Figure 4B**). Results could be obtained within five days. These cases did not respond to standard of care drugs on the platform (dexamethasone, vincristine, doxorubicin or mitoxantrone), but were individually sensitive to venetoclax (Patients 1, 2, 3) and panobinostat (Patient 5). Thus, drug profiling may provide important information when exploring options for patients with resistant disease.

The response to venetoclax *ex vivo* correlates with strong *in vivo* anti-leukemic activity as single agent and in combination

Given the strong *in vitro* activity of venetoclax across various ALL subtypes, including a subset of T-ALLs, BCP-ALLs, *TCF3-HLF* ALL and all *MLL-AF4* ALL cases, we tested venetoclax (n=7) *in vivo* in the xenograft model (**Figure 5A**). Several T-ALL cases responded to venetoclax *in vitro* with IC50 values in the nanomolar range (**Figure 5A**), consistent with reports describing activity in early thymic precursor ALL and T-ALL[40-42]. These results were verified by flow cytometry using 7-AAD staining to quantify cell death (**Figure S7**). As expected, the response to oral administration of venetoclax *in vivo* correlated with *in vitro* activity for three T-ALL patients with strong, intermediate and low venetoclax sensitivity. Single agent venetoclax treatment delayed leukemia progression significantly in the case with strong *in vitro* sensitivity (HR=20, IC50 <1nM and low Emax, treated vs. untreated, $p<0.005$) compared to cases with low IC50 (<100nM) but higher Emax (HR=0.07, treated vs. untreated, $p<0.005$) or high IC50 (>1μM). Additionally, complete response was detected when treating the T-VHR-03 case in mice with high leukemia burden (75% engraftment, **Figure S8**). We recently reported similar venetoclax efficacy in three *TCF3-HLF* ALL cases *in vivo*[35]; comparable correlations were obtained in two cases with *TCF3-HLF* and with *MLL*-rearranged ALL (**Figure 5A**). For all tested cases, venetoclax-induced delays in *in vivo* leukemia progression correlated with *in vitro* responses (**Figure 5B**, Spearman $\rho=-0.86$, p-value<0.05).

As with most chemotherapeutic agents, single agent venetoclax therapy is unlikely to be effective. Currently, most investigational agents will be tested in combination with a standard of care anti-leukemic regimen, including two to four drugs such as vincristine, dexamethasone, asparaginase and an anthracycline typically used for reinduction chemotherapy at relapse[38]. We detected synergy *in vitro* using co-titration experiments, but this assay is challenging when assessing a drug with such strong *in vitro* activity as venetoclax[43] (**Figure S9**, **Table S4**). As it is impossible to provide supportive care to mice after myelotoxic chemotherapy *in vivo*, we next tested the combination of venetoclax, dexamethasone and vincristine without anthracyclines (**Figure 5A**). Venetoclax or chemotherapy alone delayed leukemia progression for *TCF3-HLF* and *MLL-AF4* rearranged cases (HR=5-22, p-value<0.005). The three-drug

combination prevented leukemia progression for more than 300 days in two *TCF3-HLF* samples and in three out of five *MLL-AF4* ALL samples. Leukemia progression was significantly delayed in remaining samples.

The identification of response-predictive biomarkers, in addition to drug profiling, is important for the clinical development of BH3 mimetics. The BCL2:BCL-XL and BCL2:MCL1 ratios were suggested as biomarkers for venetoclax sensitivity in ALL[44] and in multiple myeloma[45], respectively. We determined levels of BCL2-family members by intracellular flow cytometry and Western blotting (**Figure 5C**, **Figure S10**). *In vitro* response to venetoclax neither correlated with BCL2-family protein expression levels nor BCL2:MCL1 or BCL2:BCL-XL ratios in 36 BCP-ALL and T-ALL samples tested by flow cytometry (**Figure 5C**, **Figure S11**). It will be important to perform further BH3 profiling in parallel with drug response profiling in clinical trials to establish predictive biomarkers.

Drug profiling identifies a subset within T-ALL highly responsive to dasatinib

We detected unexpected responses to the ABL1/SRC inhibitor dasatinib (IC50<100nM) in twelve (30%) T-ALL cases without the typical ABL1 kinase translocation (**Figure 6A**). Importantly, these responses were detected in both diagnostic and relapse samples from high-risk patients by MRD. Moreover, the IC50 for dasatinib in these cases was at least a tenfold lower than in any of the best BCP-ALL responders tested. These included five ALL cases with rearranged *TCF3-PBX1*, recently linked to active BCR signalling[19,46], that were sensitive to dasatinib but not imatinib (**Figure 6A**). No known recurrent genetic abnormality could be linked to this phenotype (**Table S3**). We found neither recurrent mutations nor gene fusions by exome and transcriptome sequencing that associated with dasatinib sensitivity in T-ALL (**Table S6**). RNASeq also indicated that dasatinib sensitive case had low *FYN*, but high *SRC* expression **(Figure S12).** Given that the dasatinib response did not correlate with the response to other BCR-ABL inhibitors, we hypothesized that dasatinib acts via SRC inhibition. By phospho-flow cytometry, we detected higher levels of activated, phosphorylated SRC in dasatinib-sensitive samples (**Figure 6B**); SRC phosphorylation was abrogated after exposure to dasatinib. The

SRC inhibitor KX2-391, which inhibits SRC at nanomolar concentrations[47], induced cell death in dasatinib-sensitive T-ALL cases at concentrations below 100nM (**Figure 6C**), supporting the relevance of the SRC pathway in this T-ALL subset. Apart from KX2-391, dasatinib response also correlated with responses to other RTK inhibitors (e.g. midostaurin, crenolinib, adj. p-value<0.005; **Figure S13**), consistent with the central role of SRC in receptor tyrosine kinase (RTK) signalling[48]. Importantly, *in vitro* response to dasatinib correlated with anti-leukemic activity *in vivo* in T-ALL xenografts (**Figure 6D**).

To validate our observations, we checked the drug sensitivity of 33 adult and pediatric T-ALL patients obtained on a liquid monoculture platform[18]. Remarkably, 4/33 responded to dasatinib with IC50 < 10nM (**Figure 6E**), and 9/33 with 10 nM < IC50 < 100nM. One of these samples was from an adult male patient with refractory T-ALL with mediastinal and abdominal lymph node involvement after 8 cycles of hyper CVAD chemotherapy, allogeneic stem cell transplantation, and relapse treatment with nelarabine, mitoxantrone and cytarabine. Based on these results, dasatinib (140 mg/day) was initiated, first in combination with pegylated asparaginase, which was interrupted after one dose due to intolerance. Dasatinib monotherapy was continued and interval resolution of all lesions was evidenced on a repeat PET/CT two month after initiation of dasatinib (**Figure 6F**). In total, the disease could be controlled over 5 months. While the short exposure to asparaginase may have contributed to this response, the disease control with dasatinib monotherapy over several months is indicative of clinical activity. These results confirm that a subset of drug resistant and relapsed T-ALL can be identified by drug profiling to be particularly sensitive to dasatinib, and warrants further exploration of underlying molecular mechanisms. Given the experience with established combinations of dasatinib with chemotherapy for the treatment of BCR-ABL positive ALL[49], our data provide a strong rationale for drug repurposing based on drug profiling results for selected patients with resistant T-ALL in pediatric and adult patient populations.

DISCUSSION

Here we provide compelling evidence that informative and reproducible differences in drug response profiles can be detected in patient groups of interest while simultaneously revealing patient-to-patient response variations. Heterogeneous and strong activity was found for different classes of agents in refractory ALL cases. We did not observe any correlations between drug response phenotypes and somatic mutations, which may be partly due to the limited size of our cohort; multivariate analyses based on whole genome or exome sequencing results on a larger cohort would be of interest in the future to establish correlations definitively. However, our results, which indicate that it will be challenging to infer drug activity solely based on genomic data, are consistent with reports in adult hematologic malignancies[16,18].

As a basis for standardization, we opted for co-culture on human MSC[27,28], which efficiently supported most of the primary ALL samples that we tested in serum-free conditions. Our assay provides better ALL cell survival and stronger correlation with in-vivo drug activity in PDX models compared to monocultures (**Figure S5**). This model also increases the possibilities for multidimensional expansion. Effects can be analysed not only on the target leukemia cells, but also on non-hematopoietic microenvironmental cells, and use of additional markers that indicate for instance metabolic states, distinct differentiation processes or signalling activity could be envisaged. The fact that we detect subsets with more proliferative activity both *in vitro* and *in vivo* based on drug profiling indicates that important leukemia-intrinsic features are maintained and captured under the *in vitro* cell culture conditions. We and others[16,18] have demonstrated the use of drug profiling for the identification of responsive phenotypes to new therapeutic agents. We have identified recurrent ALL cases highly sensitive to triggering RIP1-dependent cell death with SMAC mimetics[37], or to BCL2 inhibition in BCP-ALL subsets, including *TCF3-HLF* ALL[35] and T-ALL subsets. Moreover, we discovered a subgroup in T-ALL that is highly sensitive to dasatinib, which should be further evaluated first in patients with highly resistant and refractory disease.

Drug response profiling may contribute to defining cohorts that may benefit from new agents. The profiles that we detected for venetoclax[30], which was recently approved for CLL treatment, illustrate the type of information that could be used to improve patient selection in early clinical trials. We show that a relatively large proportion of BCP-ALL cases may respond to venetoclax, including very high-risk subtypes such as *TCF3-HLF*[35] and *MLL-AF4* positive ALL. Our findings are confirmed independently by others, showing strong venetoclax activity in MLL-rearranged ALL[50]. Supportive information using other biomarkers would be desirable, also to monitor response in clinical trials. The BCL2:BCL-XL expression ratio was proposed as a predictive biomarker for venetoclax response[44], but our results and other data[50] suggest that this approach may not detect all cases. BH3 profiling using synthetic peptides instead of targeted small molecule drugs[44,51,52] may provide complementary information, as evaluated in a phase II study assessing venetoclax monotherapy in patients with refractory/relapsed AML [53]. We propose that *in vitro* drug profiling should be incorporated in upcoming clinical trials, for example for venetoclax, in order to determine its predictive potential.

New treatment options are urgently needed for relapsed T-ALL[1]. We discovered a T-ALL subset highly sensitive to dasatinib. We also show good response to this tyrosine kinase inhibitor in a patient with previously refractory T-ALL whose treatment was designed based on drug profiling data. A patient with *NUP1-ABL1* positive T-ALL was also reported to respond to dasatinib-based therapy[54], but none of the cases with high dasatinib sensitivity were *NUP1-ABL1* positive in our series. We did not identify activating mutations that may directly explain dasatinib sensitivity, indicating that the underlying mechanisms may occur at a different level, which will motivate follow-up studies. Given that dasatinib combinations with ALL standard of care chemotherapy[49] and a pediatric dose[55] are established, its inclusion in chemotherapy for patients with resistant T-ALL displaying a dasatinib-responsive phenotype should be evaluated. Taken together, we demonstrate that *in vitro* drug profiling captures functional information of clinical importance and reveals new biological entities in ALL. Given the growing interest of clinicians in this approach, prospective evaluation is warranted to establish its value for more precise therapeutic agent selection for patients with resistant disease.

ACKNOWLEDGMENTS

This work was supported by the Cancer League of the Canton of Zurich, the Empiris foundation, the foundation “Kinderkrebsforschung Schweiz”, the Sassella foundation, the “Stiftung für Krebsbekämpfung”, the Swiss National Science Foundation (310030-133108), the Fondation Panacee, the clinical research focus program “Human Hemato-Lymphatic Diseases” of the University of Zurich, the German Childhood Cancer Foundation and the German Cancer Consortium. P.H. acknowledges support from the Hungarian National Brain Research Program (MTA-SE-NAP B-BIOMAG) and the Finnish TEKES FiDiPro Fellow Grant 40294/13. J.W.T. is supported by The Leukemia & Lymphoma Society, the V Foundation for Cancer Research, the Gabrielle’s Angel Foundation for Cancer Research, and the National Cancer Institute (5R00CA151457-04; 1R01CA183947-01). This research received funding from the European Union’s Seventh Framework Programme for research, technological development, and demonstration (Grant agreement no. 278514 - IntReALL). V.S. is a Wellcome-DBT Margdarshi Fellow. M.P.D. is a SystemsX fellow. M.P.D. wishes to thank Dr. Edoardo Missiaglia for helpful discussions.

AUTHORSHIP CONTRIBUTIONS

J.-P.B., B.C.B., V.F., M.P.D., A.R. jointly designed the project. J.-P.B., B.C.B., J.W.T., V.F., A.R., S.H.D. designed experiments. V.F., A.R., J.T., J.K., P.R.-P., P.V., O.P., S.J., B.M., S.H., J.W.T., S.E., S.H.D. performed experiments. G.C., M.Sc., M.St., M.P.D., T.R., P.V., M.D., A.E.K., M.U.M., A.v.S., C.E., B.H.C., T.J.B., R.H.C., S.U., P.B., O.R.B., E.D.-F., M.L.L., E.D.-F., J.T., R.M., V.S., J.A.I., T.R., T.B., R.H.C., S.D. provided reagents, analysis tools, samples and clinical data. M.P.D., V.F., A.R., P.R.-R., J.K., J.W.T., O.P. S.J. S.H.D., analysed data and prepared tables and figures. J.-P.B., B.C.B. supervised research. J.-P.B., B.C.B., M.P.D., V.F. wrote the manuscript. All authors critically reviewed the manuscript for its content.

CONFLICT OF INTEREST DISCLOSURES

T.R. is a full-time employee of Novartis Pharma AG. The remaining authors declare no competing financial interests.

The online version of the article contains a data supplement.

References

1. Locatelli F, Schrappe M, Bernardo ME, Rutella S. How I treat relapsed childhood acute lymphoblastic leukemia. *Blood*. 2012;120(14):2807-2816.
2. Inaba H, Greaves M, Mullighan CG. Acute lymphoblastic leukaemia. *Lancet*. 2013.
3. Roberts KG, Li Y, Payne-Turner D, et al. Targetable kinase-activating lesions in Ph-like acute lymphoblastic leukemia. *N Engl J Med*. 2014;371(11):1005-1015.
4. Holmfeldt L, Wei L, Diaz-Flores E, et al. The genomic landscape of hypodiploid acute lymphoblastic leukemia. *Nature genetics*. 2013;45(3):242-252.
5. Shochat C, Tal N, Bandapalli OR, et al. Gain-of-function mutations in interleukin-7 receptor-alpha (IL7R) in childhood acute lymphoblastic leukemias. *J Exp Med*. 2011;208(5):901-908.
6. Hunger SP, Devaraj PE, Foroni L, Secker-Walker LM, Cleary ML. Two types of genomic rearrangements create alternative E2A-HLF fusion proteins in t(17;19)-ALL. *Blood*. 1994;83(10):2970-2977.
7. Eckert C, Hagedorn N, Sramkova L, et al. Monitoring minimal residual disease in children with high-risk relapses of acute lymphoblastic leukemia: prognostic relevance of early and late assessment. *Leukemia*. 2015;29(8):1648-1655.
8. Bader P, Kreyenberg H, von Stackelberg A, et al. Monitoring of Minimal Residual Disease After Allogeneic Stem-Cell Transplantation in Relapsed Childhood Acute Lymphoblastic Leukemia Allows for the Identification of Impending Relapse: Results of the ALL-BFM-SCT 2003 Trial. *J Clin Oncol*. 2015.
9. Schrappe M, Hunger SP, Pui CH, et al. Outcomes after induction failure in childhood acute lymphoblastic leukemia. *N Engl J Med*. 2012;366(15):1371-1381.
10. Garnett MJ, Edelman EJ, Heidorn SJ, et al. Systematic identification of genomic markers of drug sensitivity in cancer cells. *Nature*. 2012;483(7391):570-575.
11. Barretina J, Caponigro G, Stransky N, et al. The Cancer Cell Line Encyclopedia enables predictive modelling of anticancer drug sensitivity. *Nature*. 2012;483(7391):603-607.
12. Gao H, Korn JM, Ferretti S, et al. High-throughput screening using patient-derived tumor xenografts to predict clinical trial drug response. *Nat Med*. 2015;advance online publication.
13. Wang K, Sanchez-Martin M, Wang X, et al. Patient-derived xenotransplants can recapitulate the genetic driver landscape of acute leukemias. *Leukemia*. 2016.
14. Townsend EC, Murakami MA, Christodoulou A, et al. The Public Repository of Xenografts Enables Discovery and Randomized Phase II-like Trials in Mice. *Cancer Cell*. 2016;29(4):574-586.
15. Jones L, Carol H, Evans K, et al. A review of new agents evaluated against pediatric acute lymphoblastic leukemia by the Pediatric Preclinical Testing Program. *Leukemia*. 2016;30(11):2133-2141.
16. Pemovska T, Kontro M, Yadav B, et al. Individualized systems medicine strategy to tailor treatments for patients with chemorefractory acute myeloid leukemia. *Cancer Discov*. 2013;3(12):1416-1429.
17. Pemovska T, Johnson E, Kontro M, et al. Axitinib effectively inhibits BCR-ABL1(T315I) with a distinct binding conformation. *Nature*. 2015;519(7541):102-105.
18. Tyner JW, Yang WF, Bankhead A, 3rd, et al. Kinase pathway dependence in primary human leukemias determined by rapid inhibitor screening. *Cancer Res*. 2013;73(1):285-296.
19. Geng H, Hurtz C, Lenz KB, et al. Self-Enforcing Feedback Activation between BCL6 and Pre-B Cell Receptor Signaling Defines a Distinct Subtype of Acute Lymphoblastic Leukemia. *Cancer Cell*. 2015;27(3):409-425.

20. Mihara K, Imai C, Coustan-Smith E, et al. Development and functional characterization of human bone marrow mesenchymal cells immortalized by enforced expression of telomerase. *Br J Haematol*. 2003;120(5):846-849.
21. Boutter J, Huang Y, Marovca B, et al. Image-based RNA interference screening reveals an individual dependence of acute lymphoblastic leukemia on stromal cysteine support. *Oncotarget*. 2014;5(22):11501-11512.
22. Bonapace L, Bornhauser BC, Schmitz M, et al. Induction of autophagy-dependent necroptosis is required for childhood acute lymphoblastic leukemia cells to overcome glucocorticoid resistance. *J Clin Invest*. 2010;120(4):1310-1323.
23. Schmitz M, Breithaupt P, Scheidegger N, et al. Xenografts of highly resistant leukemia recapitulate the clonal composition of the leukemogenic compartment. *Blood*. 2011;118(7):1854-1864.
24. Mirkowska P, Hofmann A, Sedek L, et al. Leukemia surfaceome analysis reveals new disease-associated features. *Blood*. 2013;121(25):e149-159.
25. Den Boer ML, Harms DO, Pieters R, et al. Patient stratification based on prednisolone-vincristine-asparaginase resistance profiles in children with acute lymphoblastic leukemia. *J Clin Oncol*. 2003;21(17):3262-3268.
26. Hartwell KA, Miller PG, Mukherjee S, et al. Niche-based screening identifies small-molecule inhibitors of leukemia stem cells. *Nat Chem Biol*. 2013;9(12):840-848.
27. Manabe A, Coustan-Smith E, Behm FG, Raimondi SC, Campana D. Bone marrow-derived stromal cells prevent apoptotic cell death in B-lineage acute lymphoblastic leukemia. *Blood*. 1992;79(9):2370-2377.
28. Iwamoto S, Mihara K, Downing JR, Pui CH, Campana D. Mesenchymal cells regulate the response of acute lymphoblastic leukemia cells to asparaginase. *J Clin Invest*. 2007;117(4):1049-1057.
29. Moorman AV. New and emerging prognostic and predictive genetic biomarkers in B-cell precursor acute lymphoblastic leukemia. *Haematologica*. 2016;101(4):407-416.
30. Souers AJ, Leverson JD, Boghaert ER, et al. ABT-199, a potent and selective BCL-2 inhibitor, achieves antitumor activity while sparing platelets. *Nat Med*. 2013;19(2):202-208.
31. Luo FR, Yang Z, Camuso A, et al. Dasatinib (BMS-354825) pharmacokinetics and pharmacodynamic biomarkers in animal models predict optimal clinical exposure. *Clin Cancer Res*. 2006;12(23):7180-7186.
32. McMillin DW, Negri JM, Mitsiades CS. The role of tumour-stromal interactions in modifying drug response: challenges and opportunities. *Nat Rev Drug Discov*. 2013;12(3):217-228.
33. Irving J, Matheson E, Minto L, et al. Ras pathway mutations are prevalent in relapsed childhood acute lymphoblastic leukemia and confer sensitivity to MEK inhibition. *Blood*. 2014;124(23):3420-3430.
34. Hof J, Krentz S, van Schewick C, et al. Mutations and deletions of the TP53 gene predict nonresponse to treatment and poor outcome in first relapse of childhood acute lymphoblastic leukemia. *J Clin Oncol*. 2011;29(23):3185-3193.
35. Fischer U, Forster M, Rinaldi A, et al. Genomics and drug profiling of fatal TCF3-HLF-positive acute lymphoblastic leukemia identifies recurrent mutation patterns and therapeutic options. *Nat Genet*. 2015;47(9):1020-1029.
36. Conter V, Bartram CR, Valsecchi MG, et al. Molecular response to treatment redefines all prognostic factors in children and adolescents with B-cell precursor acute lymphoblastic leukemia: results in 3184 patients of the AIEOP-BFM ALL 2000 study. *Blood*. 2010;115(16):3206-3214.
37. McComb S, Aguade-Gorgorio J, Harder L, et al. Activation of concurrent apoptosis and necroptosis by SMAC mimetics for the treatment of refractory and relapsed ALL. *Sci Transl Med*. 2016;8(339):339ra370.

38. Parker C, Waters R, Leighton C, et al. Effect of mitoxantrone on outcome of children with first relapse of acute lymphoblastic leukaemia (ALL R3): an open-label randomised trial. *Lancet*. 2010;376(9757):2009-2017.
39. Liedtke M, Cleary ML. Therapeutic targeting of MLL. *Blood*. 2009;113(24):6061-6068.
40. Alford SE, Kothari A, Loeff FC, et al. BH3 inhibitor sensitivity and Bcl-2 dependence in primary acute lymphoblastic leukemia cells. *Cancer Res*. 2015.
41. Suryani S, Carol H, Chonghaile TN, et al. Cell and Molecular Determinants of In Vivo Efficacy of the BH3 Mimetic ABT-263 against Pediatric Acute Lymphoblastic Leukemia Xenografts. *Clin Cancer Res*. 2014.
42. Peirs S, Matthijssens F, Goossens S, et al. ABT-199 mediated inhibition of BCL-2 as a novel therapeutic strategy in T-cell acute lymphoblastic leukemia. *Blood*. 2014;124(25):3738-3747.
43. Chou TC. Drug combination studies and their synergy quantification using the Chou-Talalay method. *Cancer Res*. 2010;70(2):440-446.
44. Chonghaile TN, Roderick JE, Glenfield C, et al. Maturation stage of T-cell acute lymphoblastic leukemia determines BCL-2 versus BCL-XL dependence and sensitivity to ABT-199. *Cancer Discov*. 2014;4(9):1074-1087.
45. Punnoose EA, Leverson JD, Peale F, et al. Expression Profile of BCL-2, BCL-XL, and MCL-1 Predicts Pharmacological Response to the BCL-2 Selective Antagonist Venetoclax in Multiple Myeloma Models. *Mol Cancer Ther*. 2016;15(5):1132-1144.
46. Bicocca VT, Chang BH, Masouleh BK, et al. Crosstalk between ROR1 and the Pre-B cell receptor promotes survival of t(1;19) acute lymphoblastic leukemia. *Cancer Cell*. 2012;22(5):656-667.
47. Fallah-Tafti A, Foroumadi A, Tiwari R, et al. Thiazolyl N-benzyl-substituted acetamide derivatives: synthesis, Src kinase inhibitory and anticancer activities. *Eur J Med Chem*. 2011;46(10):4853-4858.
48. Hynes NE, Lane HA. ERBB receptors and cancer: the complexity of targeted inhibitors. *Nat Rev Cancer*. 2005;5(5):341-354.
49. Foa R, Vitale A, Vignetti M, et al. Dasatinib as first-line treatment for adult patients with Philadelphia chromosome-positive acute lymphoblastic leukemia. *Blood*. 2011;118(25):6521-6528.
50. Khaw SL, Suryani S, Evans K, et al. Venetoclax responses of pediatric ALL xenografts reveal MLLr ALL sensitivity, but overall requirement to target both BCL2 and BCLXL. *Blood*. 2016.
51. Ni Chonghaile T, Sarosiek KA, Vo TT, et al. Pretreatment mitochondrial priming correlates with clinical response to cytotoxic chemotherapy. *Science*. 2011;334(6059):1129-1133.
52. Montero J, Sarosiek KA, DeAngelo JD, et al. Drug-induced death signaling strategy rapidly predicts cancer response to chemotherapy. *Cell*. 2015;160(5):977-989.
53. Konopleva M, Pollyea DA, Potluri J, et al. Efficacy and Biological Correlates of Response in a Phase II Study of Venetoclax Monotherapy in Patients with Acute Myelogenous Leukemia. *Cancer Discov*. 2016.
54. Deenik W, Beverloo HB, van der Poel-van de Luytgaarde SC, et al. Rapid complete cytogenetic remission after upfront dasatinib monotherapy in a patient with a NUP214-ABL1-positive T-cell acute lymphoblastic leukemia. *Leukemia*. 2009;23(3):627-629.
55. Zwaan CM, Rizzari C, Mechinaud F, et al. Dasatinib in children and adolescents with relapsed or refractory leukemia: results of the CA180-018 phase I dose-escalation study of the Innovative Therapies for Children with Cancer Consortium. *J Clin Oncol*. 2013;31(19):2460-2468.

Table 1. Characteristics of the five patients with refractory disease included in this study

FIGURE LEGENDS

Figure 1. Setup of drug response profiling platform.

Patient material, notably from high-risk cases, including relapse cases and cases with translocations linked to poor survival, were prioritized for patient-derived xenograft (PDX) and drug response profiling; PDX stability was evaluated against primary material by comparing targeted deep-sequenced leukemogenesis markers (**A**, top panel). Drug profiling was performed on primary ALL cells in co-culture with mesenchymal bone marrow stroma cells (MSCs). Automated microscopy-based image analysis was used to quantify living ALL and generate dose response curves. Imaging results are analysed with a toolkit that performs dose response normalization, outlier removal, rapid curve fitting, and extraction of response parameters (IC50, AUC, Emax). Selected single compounds and combinations are validated in the xenograft model. This platform enables the identification of drug response phenotypes in individual ALL cases, providing an additional layer of information to facilitate individual treatment approaches (**A**, bottom panel). Our PDX model preserves an average of 74% of the mutations and indels initially detected in patients, making it an ideal source of material for drug response testing in multi-center, co-clinical settings (**B**).

Figure 2. Drug response profiles of BCP-ALL and T-ALL.

Heatmap indicating the response of BCP-ALL (n=44) and T-ALL (n=24) to 60 compounds and represented by IC50 values. Samples (rows) were ordered according to clinical classification and compounds (columns) according to activity. Each compound's IC50 distribution range is shown on the lower panel forming drug clusters:

A: Generally active drugs, mean IC50 values < 10 nM;

B: Drugs more active in BCP-ALLs than T-ALLs;

C: Generally active drugs, IC50 values < 100 nM;

D: Drugs with variable activity

E: Drugs with activity linked to cycling activity;

F: Generally active drugs, high nanomolar range;

G: Generally inactive drugs, with sporadic exceptions.

On the lower part of the graph heatmap of MSC and drug IC50 distribution box plot are demonstrated.

Figure 3. Drug profiling reveals leukemia-intrinsic features.

(**A**) Co-culturing on MSC supports survival of T-ALL (n=22) and BCP-ALL (n=25). Data at day 4 are given, normalized to seeded viable cell numbers at day 0 both in monoculture or in co-culture (left panel). Cell cycle and apoptosis rates of primary T-ALL (n=18) and BCP-ALL (n=14) cells in co-culture is provided on the right. Samples are ranked from highest (top) to lowest (bottom) survival. Ratio of cells in S-phase and apoptosis is given on the far right. ****, *p<0.0001 (Paired t-test)*

(**B**) Engraftment kinetics for ALL cases with >40% of cells in S-phase (dotted lines in red) and with <40% in S-phase (straight blue lines) are given (**i.**). Time to engraftment with 25% ALL blasts in the two groups is indicated in the lower panel (**ii.**). ***, *p<0.001 (Two-sided t-test)*

(**C**) *In vitro* ALL proliferation correlates with drug response to cytarabine (antimetabolite), docetaxel (antimitotic) and other cell cycle targeting drugs (**Figure S4**). ALL cells with >40% of cells in S-phase (red symbols) respond to cytarabine and docetaxel with lower IC50 compared to samples with <40% of cells in S-phase (blue symbols).

(**D**) Cytarabine and docetaxel response profiles predict *in vivo* ALL response (N=8).

Figure 4. Distinct drug activity patterns can be detected for individual samples and patient groups of interest

(**A**) Refractory relapse (RR (PDX), N=12) samples exhibit general resistance to conventional clinical compounds, but remain sensitive to some experimental drugs.

(**C**) Primary refractory relapse patients (RR (primary), N=5) tested before last salvage therapy demonstrate persistent resistance to standard chemotherapy and individual sensitivity to experimental molecules.

All responses are represented as IC50 (log[nM]) and compared to other diagnostic and relapse ALL cases depicted in the background. **, p<0.05; **, p<0.005 (Two-sided t-test)*

Figure 5. *In vitro* sensitivity to the BCL-2 antagonist venetoclax correlates with the response in leukemia xenografts.

(**A**) *In vitro* response to venetoclax for indicated ALL subtypes (black) compared to other ALL (grey). From top to bottom: mature-T-ALL (N=6), cortical-T-ALL (N=13), pre-T-ALL (N=6), *TCF3-HLF* ALL (N=4) and *MLL-AF4* ALL (N=3). Cell viability (7-AAD) was measured by flow cytometry after treatment for 72 hours and normalized against DMSO-treated controls. Arrows indicate samples whose response had been validated *in vivo* for venetoclax (top to bottom: T-VHR-03, T-HR-11 and T-HR-10) or venetoclax in combination with vincristine and dexamethasone (top to bottom: B-HR-24, B-HR-20, B-HR-26 and B-VHR-07). The left panel shows the number of leukemia cells compared to mouse lymphocytes over time. The right panel shows corresponding Kaplan-Meier survival curves (event defined as 25% of $mCD45^-$ $hCD45^+hCD19^+$ or $hCD7^+$ leukemia cells detected by flow cytometry).

(**B**) *In vitro* response to venetoclax correlates with fold increase of survival comparing treatment with venetoclax and vehicle (N=7).

(**C**) BCL2 protein family expression (**i.**) analysed by flow cytometer in T-ALL (N=16) and BCP-ALL (N=20). Correlation of BCL2:BCL-XL and BCL2:MCL1 ratio (**ii.**) with *in vitro* venetoclax response. *****, p<0.0001 (two-tailed t test)*.

Figure 6. *In vitro* sensitivity of T-ALL to dasatinib correlates with anti-leukemic efficacy in the patient.

(**A**) Subset of T-ALL cases at diagnosis that relapsed (R) and at relapse are highly sensitive to dasatinib *in vitro*.

(**B**) Dasatinib sensitive T-ALL have higher levels of phosphorylated SRC that decreases after treatment with 1µM dasatinib for 2h as measured by flow cytometry. ***, *p<0.001 (Two-sided t-test)*

(**C**) Dasatinib response correlates with sensitivity to the SRC inhibitor KX2-391 (N=16).

(**D**) *In vitro* captured response correlates with *in vivo* response to dasatinib (N=10). Indicated are the % of T-ALL blasts compared to mouse lymphocytes, normalized to vehicle treated controls.

(**E**) Sensitivity of adult and pediatric T-ALL cases to dasatinib reveals 40% of cases with IC50 below 100 nM.

(**F**) Left PET/CT demonstrates significant disease burden throughout the marrow in bilateral upper and lower extremities, the pelvis, vertebrae, and contiguous nodes within the mediastinum. Right PET/CT approximately 15 months after the original presentation, shortly after initiation of dasatanib monotherapy. This image demonstrates complete response with no signs of marrow or nodal involvement.

Table 1. Characteristics of the five patients with refractory disease included in this study

Patient	Sex, age	Clinical Status at time point of drug profiling	Salvage treatment	Current status
Patient 1	F, 2	Relapsed after SCT, early relapse	MLL:MLLT10 positive, blinatumomab	alive, follow up 15 months
Patient 2	M, 7	Relapsed after SCT, second relapse, resistant to anti CD19 therapy	Blinatumomab, second transplant	alive, follow up 9 months
Patient 3	F, 8	Relapsed after SCT, second relapse	Chemotherapy, second transplant	died
Patient 4	F, 5	Very early BM relapse	Resistant to blinatumomab, no response to bortezomib + 4 drugs	died
Patient 5	F, 11	Relapsed after SCT, second (late) relapse	Second transplant, resistant to blinatumomab, partial response to bortezomib + 4 drugs	died

F - female
M - male

Figure 1.

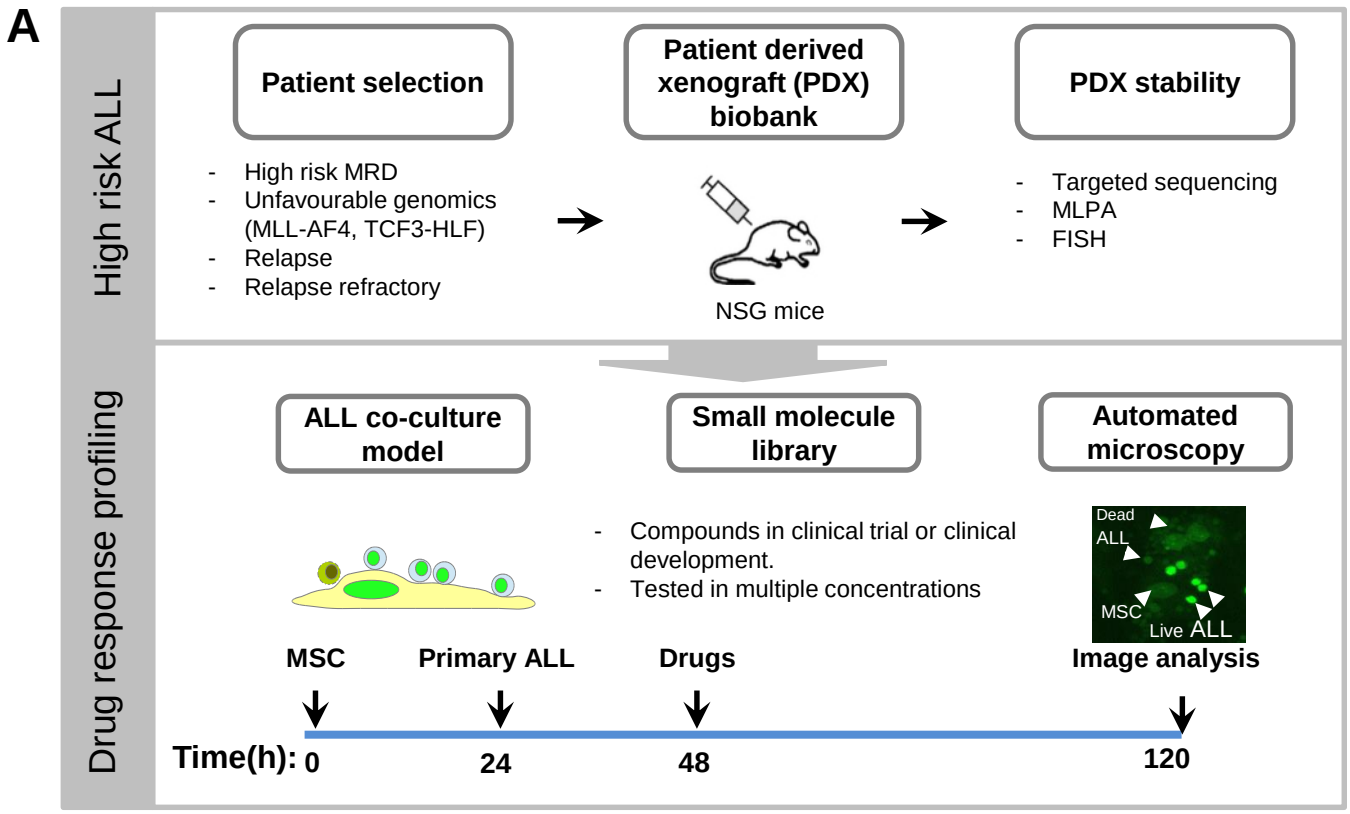
A
High risk ALL
Patient selection
- High risk MRD
- Unfavourable genomics (MLL-AF4, TCF3-HLF)
- Relapse
- Relapse refractory
Patient derived xenograft (PDX) biobank
NSG mice
PDX stability
- Targeted sequencing
- MLPA
- FISH
Drug response profiling
ALL co-culture model
Small molecule library
- Compounds in clinical trial or clinical development.
- Tested in multiple concentrations
Automated microscopy
Dead
ALL
MSC
Live ALL
MSC
Primary ALL
Drugs
Image analysis
Time(h): 0
24
48
120

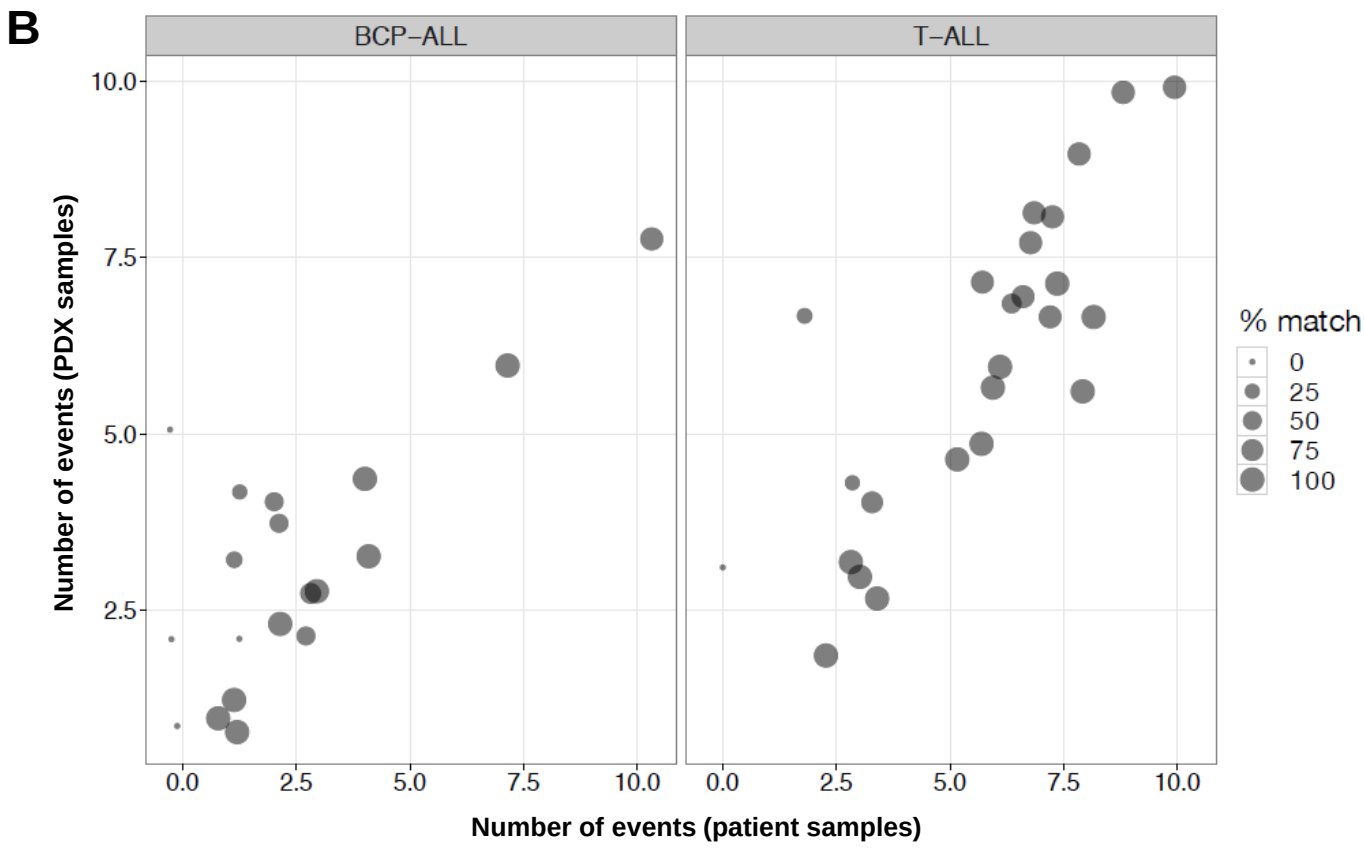
B
BCP–ALL
T–ALL
Number of events (PDX samples)
Number of events (patient samples)
0.0
2.5
5.0
7.5
10.0
% match
0
25
50
75
100

Figure 2.

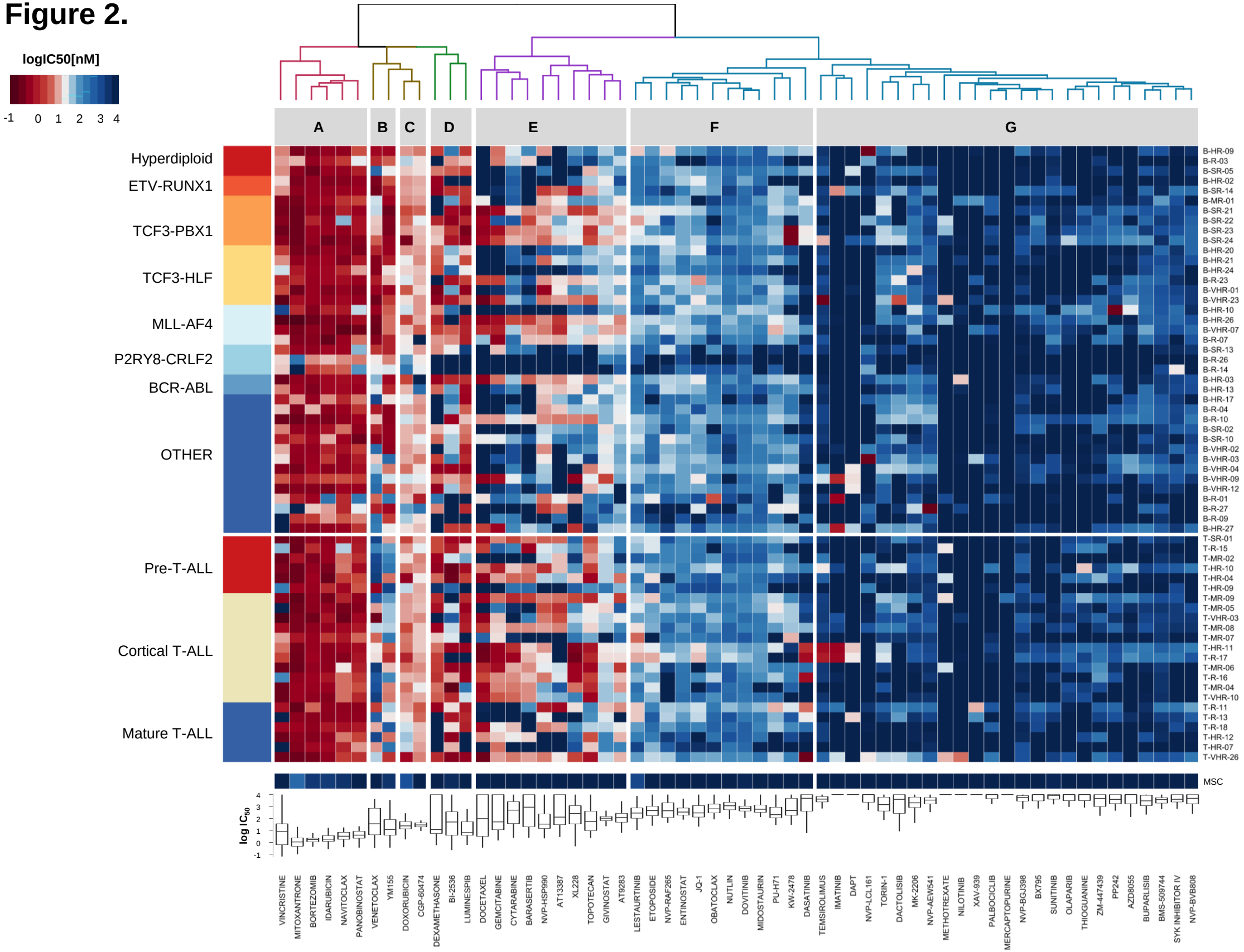
logIC50[nM]
-1 0 1 2 3 4
A
B
C
D
E
F
G
Hyperdiploid
ETV-RUNX1
TCF3-PBX1
TCF3-HLF
MLL-AF4
P2RY8-CRLF2
BCR-ABL
OTHER
Pre-T-ALL
Cortical T-ALL
Mature T-ALL
B-HR-09
B-R-03
B-SR-05
B-HR-02
B-SR-14
B-MR-01
B-SR-21
B-SR-22
B-SR-23
B-SR-24
B-HR-20
B-HR-21
B-HR-24
B-R-23
B-VHR-01
B-VHR-23
B-HR-10
B-HR-26
B-VHR-07
B-R-07
B-SR-13
B-R-26
B-R-14
B-HR-03
B-HR-13
B-HR-17
B-R-04
B-R-10
B-SR-02
B-SR-10
B-VHR-02
B-VHR-03
B-VHR-04
B-VHR-09
B-VHR-12
B-R-01
B-R-27
B-R-09
B-HR-27
T-SR-01
T-R-15
T-MR-02
T-HR-10
T-HR-04
T-HR-09
T-MR-09
T-MR-05
T-VHR-03
T-MR-08
T-MR-07
T-HR-11
T-R-17
T-MR-06
T-R-16
T-MR-04
T-VHR-10
T-R-11
T-R-13
T-R-18
T-HR-12
T-HR-07
T-VHR-26
MSC
log IC50
4
3
2
1
0
-1
VINCRISTINE
MITOXANTRONE
BORTEZOMIB
IDARUBICIN
NAVITOCLAX
PANOBINOSTAT
VENETOCLAX
YM155
DOXORUBICIN
CGP-60474
DEXAMETHASONE
BI-2536
LUMINESPIB
DOCETAXEL
GEMCITABINE
CYTARABINE
BARASERTIB
NVP-HSP990
AT13387
XL228
TOPOTECAN
GIVINOSTAT
AT9283
LESTAURTINIB
ETOPOSIDE
NVP-RAF265
ENTINOSTAT
JQ-1
OBATOCLAX
NUTLIN
DOVITINIB
MIDOSTAURIN
PU-H71
KW-2478
DASATINIB
TEMSIROLIMUS
IMATINIB
DAPT
NVP-LCL161
TORIN-1
DACTOLISIB
MK-2206
NVP-AEW541
METHOTREXATE
NILOTINIB
XAV-939
PALBOCICLIB
MERCAPTOPURINE
NVP-BGJ398
BX795
SUNITINIB
OLAPARIB
THIOGUANINE
ZM-447439
PP242
AZD8055
BUPARLISIB
BMS-509744
SYK INHIBITOR IV
NVP-BVB808

Figure 3.

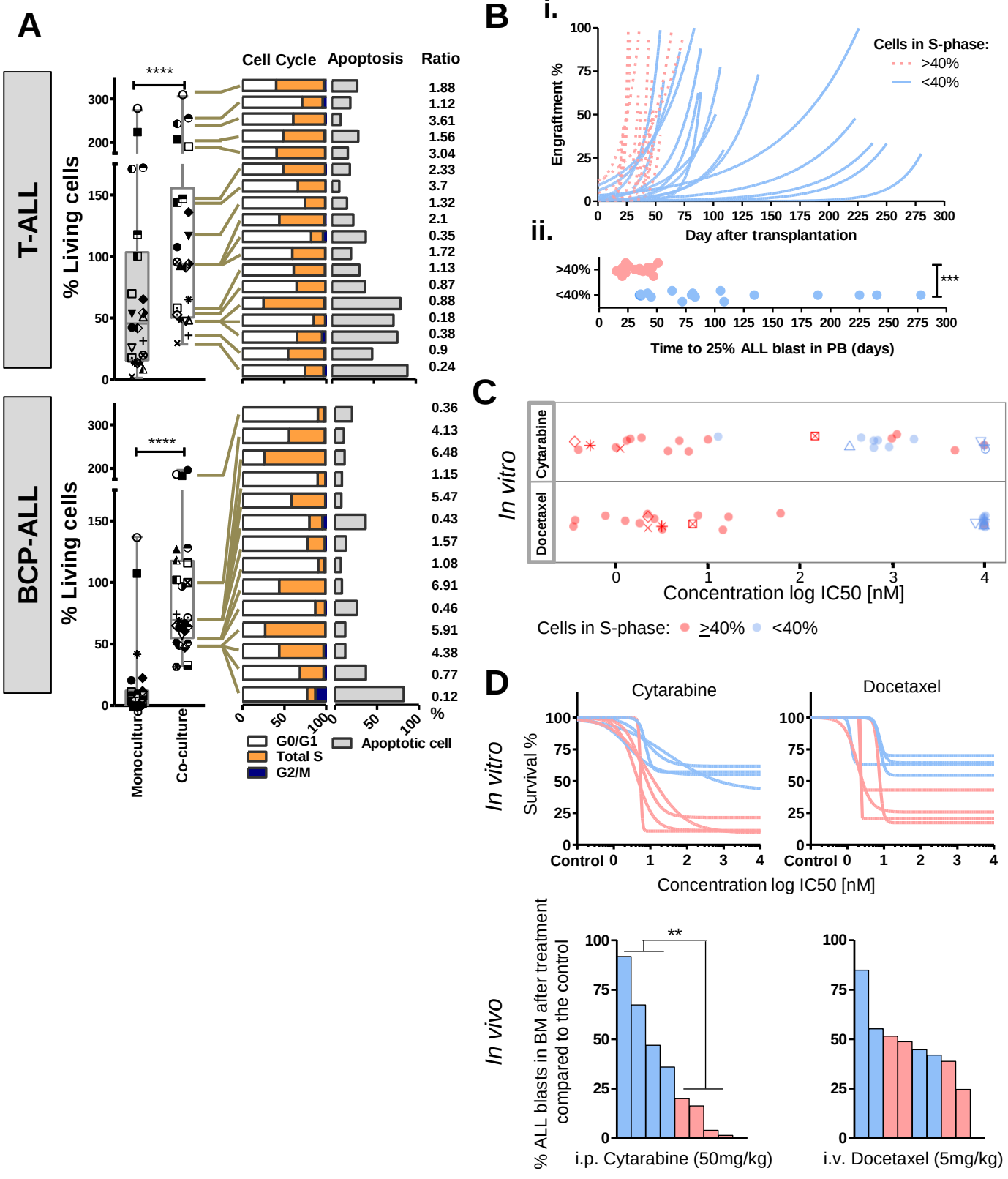
A
T-ALL
BCP-ALL
% Living cells
****
Cell Cycle
Apoptosis
Ratio
1.88
1.12
3.61
1.56
3.04
2.33
3.7
1.32
2.1
0.35
1.72
1.13
0.87
0.88
0.18
0.38
0.9
0.24
0.36
4.13
6.48
1.15
5.47
0.43
1.57
1.08
6.91
0.46
5.91
4.38
0.77
0.12
%
Monoculture
Co-culture
G0/G1
Total S
G2/M
Apoptotic cell
B
i.
Engraftment %
Day after transplantation
Cells in S-phase:
>40%
<40%
ii.
***
Time to 25% ALL blast in PB (days)
C
In vitro
Cytarabine
Docetaxel
Concentration log IC50 [nM]
Cells in S-phase: ≥40% <40%
D
In vitro
Cytarabine
Docetaxel
Survival %
Control
Concentration log IC50 [nM]
In vivo
% ALL blasts in BM after treatment compared to the control
**
i.p. Cytarabine (50mg/kg)
i.v. Docetaxel (5mg/kg)

Figure 4.

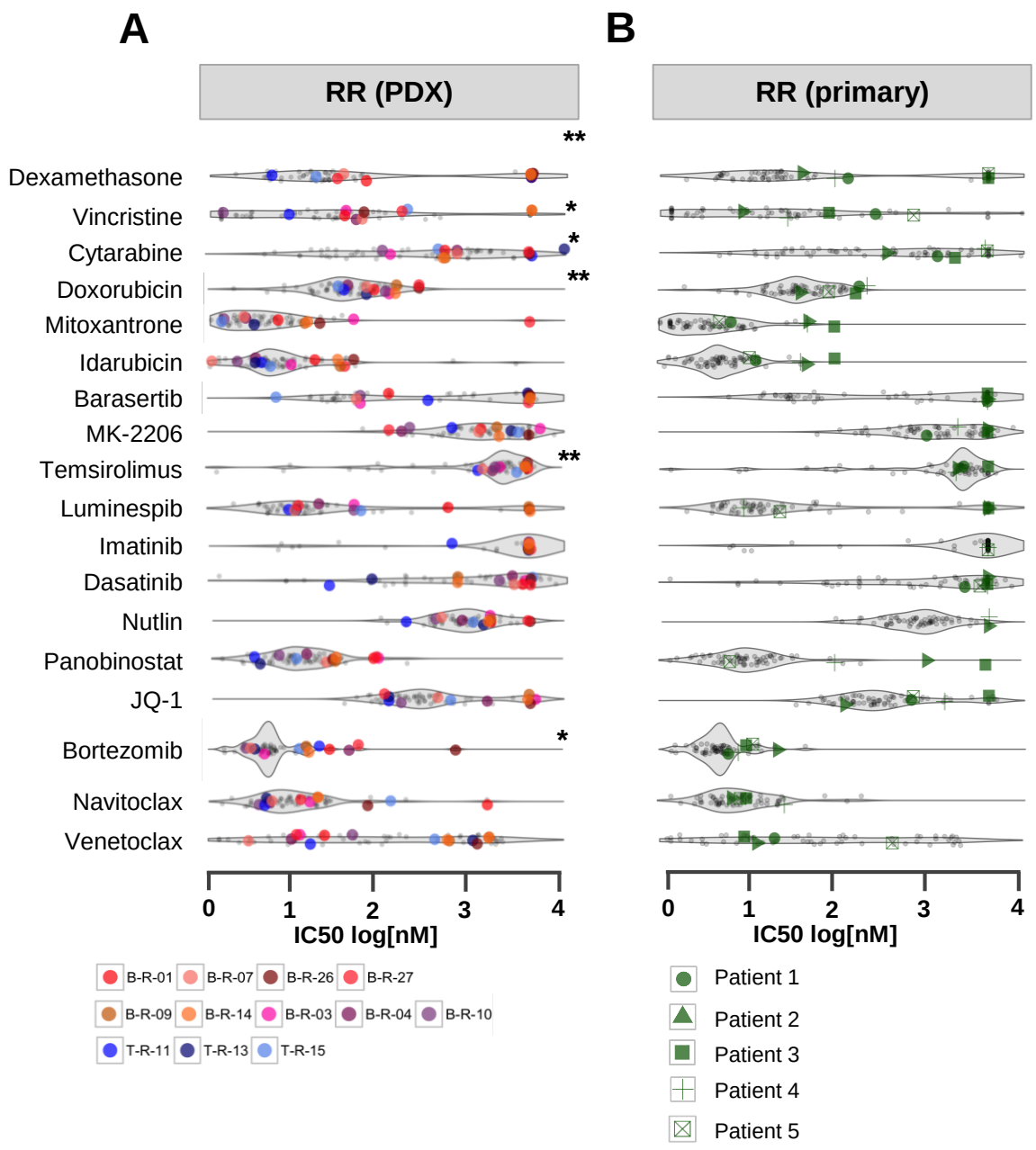
A
B
RR (PDX)
RR (primary)
Dexamethasone
Vincristine
Cytarabine
Doxorubicin
Mitoxantrone
Idarubicin
Barasertib
MK-2206
Temsirolimus
Luminespib
Imatinib
Dasatinib
Nutlin
Panobinostat
JQ-1
Bortezomib
Navitoclax
Venetoclax
**
*
*
**
**
*
0
1
2
3
4
IC50 log[nM]
B-R-01
B-R-07
B-R-26
B-R-27
B-R-09
B-R-14
B-R-03
B-R-04
B-R-10
T-R-11
T-R-13
T-R-15
Patient 1
Patient 2
Patient 3
Patient 4
Patient 5

Figure 5.

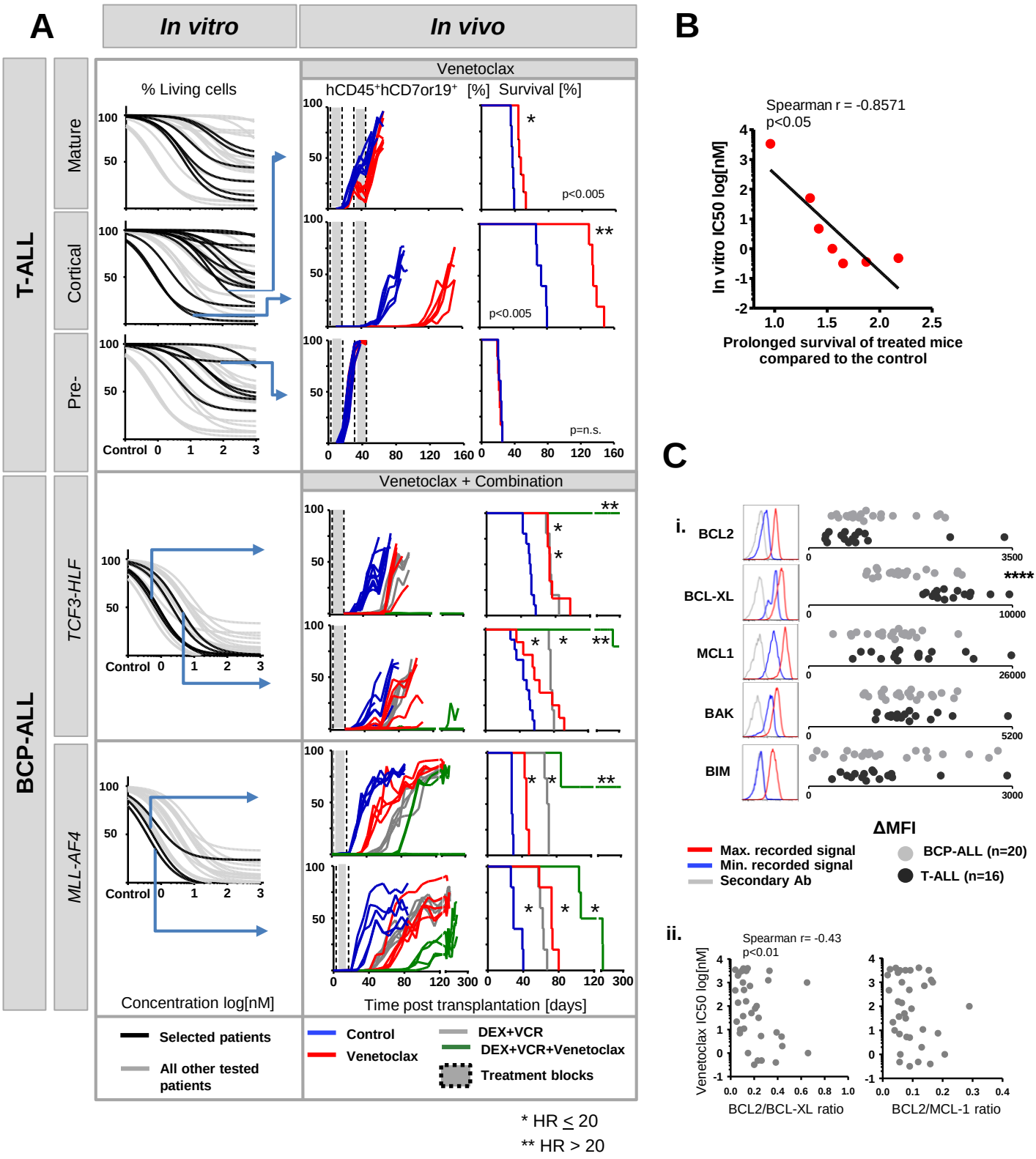
A
In vitro
In vivo
T-ALL
BCP-ALL
Mature
Cortical
Pre-
TCF3-HLF
MLL-AF4
% Living cells
Control
Concentration log[nM]
Venetoclax
hCD45+hCD7or19+ [%]
Survival [%]
p<0.005
p=n.s.
Venetoclax + Combination
Time post transplantation [days]
Selected patients
All other tested patients
Control
Venetoclax
DEX+VCR
DEX+VCR+Venetoclax
Treatment blocks
* HR ≤ 20
** HR > 20
B
Spearman r = -0.8571
p<0.05
ln vitro IC50 log[nM]
Prolonged survival of treated mice compared to the control
C
i.
BCL2
BCL-XL
MCL1
BAK
BIM
ΔMFI
Max. recorded signal
Min. recorded signal
Secondary Ab
BCP-ALL (n=20)
T-ALL (n=16)
ii.
Spearman r= -0.43
p<0.01
Venetoclax IC50 log[nM]
BCL2/BCL-XL ratio
BCL2/MCL-1 ratio

Figure 6.

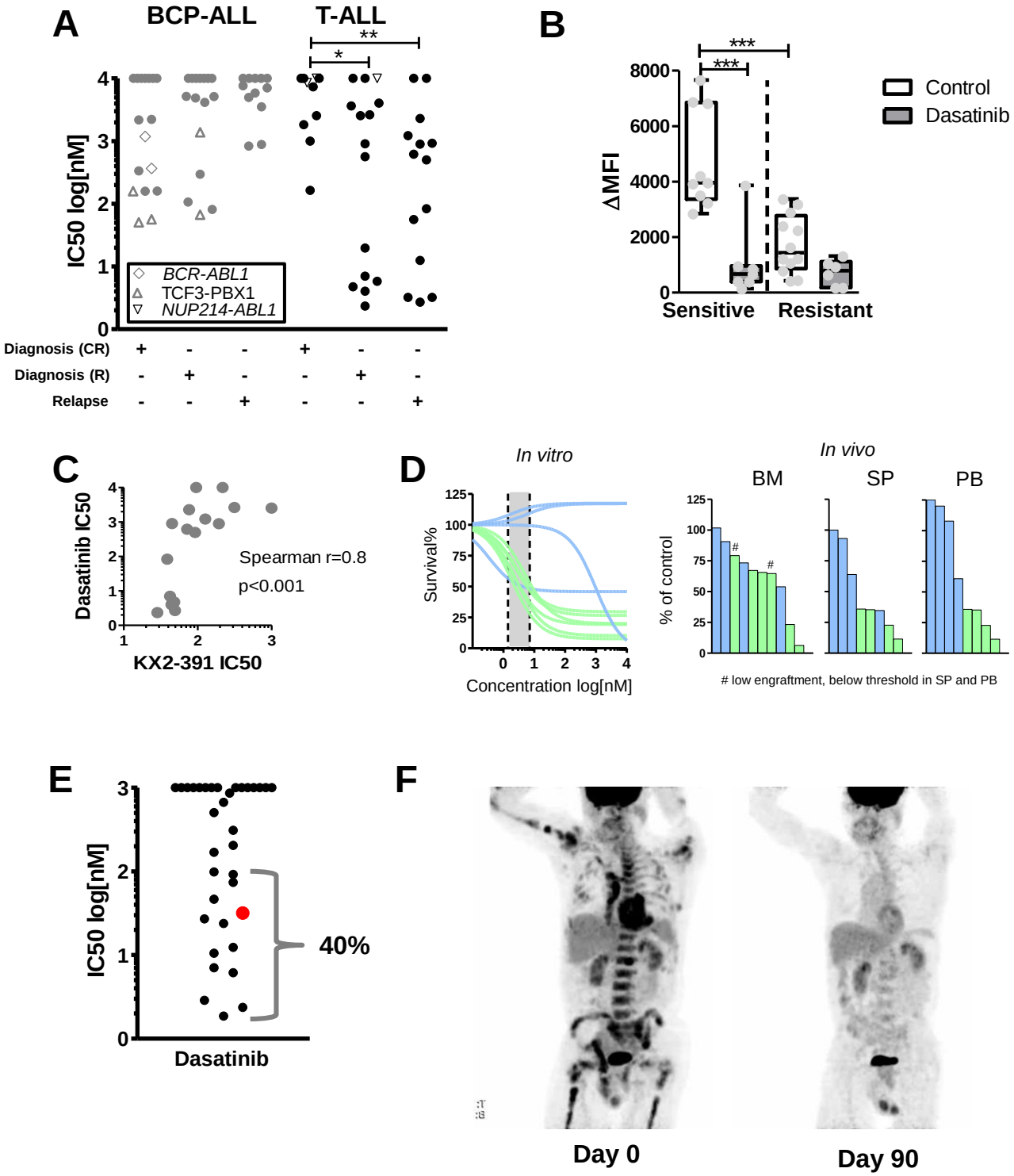
A
BCP-ALL
T-ALL
**
*
IC50 log[nM]
BCR-ABL1
TCF3-PBX1
NUP214-ABL1
Diagnosis (CR)
Diagnosis (R)
Relapse
B
***
***
ΔMFI
Control
Dasatinib
Sensitive
Resistant
C
Dasatinib IC50
KX2-391 IC50
Spearman r=0.8
p<0.001
D
In vitro
Survival%
Concentration log[nM]
In vivo
BM
SP
PB
% of control
# low engraftment, below threshold in SP and PB
E
IC50 log[nM]
40%
Dasatinib
F
Day 0
Day 90